Costa Figueiredo, Marta; Sorsa, Olli; Arán-Ais, R.M.; Doan, Nguyet; Feliu, J.M.; Kallio, Tanja

Trimetallic catalyst based on PtRu modified by irreversible adsorption of Sb for direct ethanol fuel cells

Published in:
Journal of Catalysis

DOI:
10.1016/j.jcat.2015.04.032

Published: 01/09/2015

Document Version
Peer-reviewed accepted author manuscript, also known as Final accepted manuscript or Post-print

Tri-metallic catalyst based on PtRu modified by irreversible adsorption of Sb for direct ethanol fuel cells

Marta C. Figueiredo[1, a], Olli Sorsa[1], Rosa M. Arán-Ais[2], Nguyet Doan[1], Juan M. Feliu[2], Tanja Kallio[1]

[1] *Research group of Fuel Cells, School of Chemical Technology, Aalto University, P.O. Box 16100, 00076 Aalto, Finland*

[2] *Instituto de Electroquimica, Universidad de Alicante Ap. 99, E-03080, Alicante, Spain*

A) Present address:
Leiden Institute of Chemistry - Catalysis and Surface Chemistry, Gorlaeus Laboratories
Einsteinweg 55, 2333 CC Leiden, The Netherlands

[1] Corresponding Author:
Marta C. Figueiredo; Telf.: + Tel.: +358503435167; fax:+358947022580
Department of Chemistry, School of Chemical Technology
Aalto University, FI-00076 AALTO, Finland
E-mail address: marta.figueiredo@aalto.fi

Abstract:

In this work, PtRu/C-Sb materials prepared by adding a Sb salt to the ink of commercial PtRu/C were studied as catalysts for ethanol oxidation. The prepared trimetallic catalysts showed enhanced properties for ethanol oxidation trough a wide range of surface coverages. However, coverage higher than 0.7 of Sb on PtRu/C causes the decrease of the catalytic activity suggesting that specific sites composed by the 3 metals are necessary to achieve the highest performance. In situ Fourier Transformed Infrared Spectroscopy experiments were also performed to compare the reaction products of the bimetallic and trimetallic catalysts. The catalysts were also tested under fuel cell conditions. Also in this case, higher power densities, higher open circuit voltages and better stability than the bimetallic substrate were found. With this catalyst preparation method, the catalysts showed 2 times higher current densities than for the PtRu catalysts and 6 times better than for pure Pt anodes.

Keywords: PtRu catalysts, antimony, irreversible adsorption, direct ethanol fuel cells

1. Introduction:

Direct alcohol fuel cells (DAFC) have emerged in the last decades as promising alternative power sources for mobile applications due to their low operating temperatures, higher energy density and facile storage and delivery of liquid fuels [1]. The particular case of direct ethanol fuel cell (DEFC) presents many advantages when compared with the direct methanol fuel cell (DMFC) fuelled with methanol (the most extensively studied fuel for direct alcohol fuel cells DAFC) due to its lower toxicity, higher theoretical power densities, low crossover and, especially, because ethanol can be

easily produced from biomass [1]. Ethanol is, nowadays, one of the best options for portable carbon free energy production systems. However, power densities of DEFCs are still lower than required for commercial applications especially because of the poor activity of the anode catalysts.

The desired reaction in the DEFC anodes is the complete electro-oxidation of ethanol to carbon dioxide and protons, involving the cleavage of the C-C bond and the transference of 12 electrons. However, during this process some poisoning intermediates, such as CO, can be formed and adsorb strongly on the catalysts surfaces blocking the active sites from further oxidation reactions [2-4], thus decreasing the overall performance of the catalyst and the cell.

Although Pt is considered one of the best catalysts for ethanol oxidation, it has a low ability for the C-C bond cleavage and it is easily poisoned by the intermediates that adsorb strongly on the Pt surface [5-7]. The addition of other metals (as an alloy [8-13] or by irreversible adsorption [14, 15]) to Pt has become the way of tailoring the properties of this metal in order to improve their resistance to the poison formation or its capability for breaking the C-C bonds. The higher performance of bimetallic catalysts toward ethanol oxidation has been attributed to a bifunctional mechanism and to the change of the electronic properties of Pt [16]. In the bifunctional mechanism, the oxidation of the strongly adsorbed intermediates is facilitated by the presence of foreign metal oxides that supply oxygen atoms at lower potentials than in pristine Pt. On the other hand, the presence of the foreign metal changes the electronic structure of the Pt atoms, modifying consequently its adsorption properties for the involved intermediates [5].

Within the most successful examples are PtSn [8, 9, 11] and PtRu [9, 12, 13] based catalyst. According to literature, when Ru is present in the alloy it acts as an oxygen supplier at low potentials, diminishing the poisoning effect from the metastable intermediates [7]. In the case of Sn, its presence favours

dissociative adsorption of ethanol. Colmati et al [12], suggested that the high selectivity of this type of catalyst toward the oxidation of ethanol to CO_2 is due to the facility of breaking the C-C bond at lower potentials.

Ternary alloys have also been widely studied recently [17-22]. The addition of the third component usually changes the electronic and structural properties of the alloy leading, generally to catalysts with higher activity than their mono and bimetallic precursors. Alloys such as PtRuSn [17], PtRhSn [18], PtMoIr [19], PtRuMo [20, 21] or PtSnMo [22] have been reported in the literature. In these catalysts, the presence of the oxophilic element in the alloy enhances the water oxidation, leading to the early formation of adsorbed hydroxides which act as oxidants for the strongly adsorbed intermediates. Within this ternary alloys, it was found that the higher ethanol current density was obtained from PtRuMo [20, 21]. However, the current increase has been attributed to the higher yields of C_2 products and not from the total oxidation of ethanol to CO_2. Thus, finding a catalyst improving the direct ethanol oxidation to CO_2 at low overpotentials and consequently allow the commercialization of the DEFC is still an open task.

It has been recently reported by our group, that the use of irreversible adsorption of metallic adatoms on platinum based catalysts can lead to a 3-fold increase of the fuel cell performance when compared with Pt [23]. The bimetallic catalysts, Pt/C-Bi and Pt/C-Sb showed to be better option as catalysts for both ethanol and propanol fed DAFC. The irreversible adsorption of foreigner metals for catalysts preparation presents several advantages because as a very simple method it avoids all the complicated synthesis process. In this paper we report the performance of PtRu/C catalysts modified with different amounts of irreversibly adsorbed Sb for ethanol oxidation. The experiments were also carried out in a DEFC. These trimetallic catalysts reveal an enhanced activity toward ethanol oxidation, higher power

densities, higher open circuit voltages and good stability when compared with the bimetallic substrate. With this catalyst preparation method, a good distribution of the oxophilic metal is obtained on the anode and the performance achieved is 2 times higher than for the PtRu catalysts and 6 times better than for pure Pt anodes.

2. Experimental

2.1. Electrochemical characterization

The electrochemical experiments were performed in a classical three electrode cell at controlled temperature (20^{o}C) and under nitrogen purge (AGA, 99.999%). A platinum coil was used as a counter electrode and a reversible hydrogen electrode as a reference. The working electrode was prepared by deposition of 4 µl of an ink onto a glassy carbon electrode (0.1963 cm^2 of geometric area) previously cleaned by polishing with an alumina suspension and rinsing in an ultrasonic bath [15]. The ink was prepared using 5 mg of carbon supported Pt catalyst (60% wt., Alfa Aesar) or PtRu/C (Pt 40% wt, Ru 20% wt on Vulcan from Alfa Aesar), 20 µl of Nafion® solution (5 wt. % Aldrich) and 200 µl of ethanol (p.a., Altia) that were stirrer and sonicated. The composition of the PtRu/C used as base catalysts for this study was chosen on the bases of previous reports on the effect of the Ru content on the PtRu bimetal for ethanol oxidation [24] where ~40% of Ru is shown to be the optimal content.

For the catalysts containing Sb, Pt/C- Sb or PtRu/C-Sb were prepared just by adding Sb_2O_3 salt to the ink (approximately 20% of the metal content of the catalyst). The inks were sonicated for different times (5 min to 1hour) to change the surface coverage of Sb (longer times for higher contents of Sb) [15, 23]. The electrodes prepared with this procedure have a Pt loading of ~ 0.02 mg.

The experiments were performed with a potentiostat/galvanostat PGSTAT100 Autolab system and a rotating device from Pine Instruments.

Cyclic voltammetry in 0.5 M H_2SO_4 (Merck) was done for the electrochemical characterization of the catalysts. Following the procedure previously described [24], prior to the use of the nanoparticles for alcohol oxidation, the catalysts were cleaned by CO (AGA, 99.999%) adsorption and stripping [25]. Because Sb does not adsorb H, after the cleaning the blank CVs can be used to access the relative Sb coverage according with the following equation (Equation 1).

$$\theta_{Sb} = 1 - \theta_H = \frac{q_H^0 - q_H^{Sb}}{q_H^0} \quad \text{(Equation 1)}$$

Where q_H^0 is the charge for hydrogen adsorption on the pristine PtRu/C catalyst between 0.06 and 0.32 V (vs RHE) and q_H^{Sb} is the charge for hydrogen adsorption on the modified PtRu/C-Sb electrode for a given coverage. Using this formula a good approximation on the Sb coverage can be achieved and the values are normalized for 1 (full coverage). The use of this method for quantifying the amount of Sb on the catalyst excludes the adatom adsorption on the Ru atoms. Although Sb can adsorb on Ru, the modified Ru electrode showed to be very unstable under electrochemical conditions (Figure S1A in Supporting Information) and almost no Sb remains on the Ru catalyst after 20 cycles between 0.05 and 0.8 V (vs RHE). Moreover, experiments done in the presence of ethanol showed that, even when Sb is still adsorbed on Ru/C, no oxidation of ethanol occurs (as in pure Ru) suggesting that the active catalyst is the Sb deposited on the Pt atoms (Figure S1B – Supporting Information). For these reasons, when referring to the Sb coverage, calculated from equation 1, it means the amount of Sb on Pt sites (that are the stable catalytic ones). It should also be mentioned that Sb does not adsorb on carbon (Figure S1C – Supporting Information).

The activity of the catalyst towards ethanol oxidation was measured in an electrochemical cell containing 1 M of ethanol in 0.1 M $HClO_4$ (Merck).

2.2. FTIR

Fourier-transform infrared spectroscopy (FTIRS) experiments were performed with a Nicolet Magna 850 spectrometer, equipped with an MCT detector. The spectroelectrochemical cell was provided with a prismatic CaF_2 window beveled at 60º. Spectra shown are composed of 100 interferograms collected with a resolution of 8 cm^{-1} and p-polarized light. They are presented as absorbance, according to $A = \log(R/R_0)$, where R and R_0 are the reflectance corresponding to the single beam spectra obtained at the sample and reference potentials, respectively [26]. All the spectroelectrochemical experiments were conducted at room temperature, with a reversible hydrogen electrode (RHE) and a platinum wire used as the reference and counter electrodes, respectively. For these experiments a gold collector electrode was used [15] and the inks were prepared without the ionomer (Nafion) in order to avoid the undesirable bands coming from the polymer [15, 27].

The contact of the electrodes with the ethanol solution (1M EtOH in 0.1M $HClO_4$) was performed at controlled potential (0.1 V) where, apparently, no adsorption or reaction process take place [15]. This potential was maintained until the electrode was pressed against the CaF_2 window. After collecting the reference spectrum at this potential, the potential was stepped progressively to higher potentials up to 0.8 V.

2.3. Fuel cell experiments

Prior to the fuel cell experiments, membrane electrode assembly (MEA) with Pt/C, Pt/C-Sb, PtSn/C, PtRu/C or PtRu/C-Sb as an anode and Pt/C as a cathode catalyst were prepared [23]. The PtSn/C particles were included in this study for sake of comparison and they were synthesized by water in oil microemulsion method as described elsewhere [28]. The inks for the electrodes were made by mixing the catalyst, Nafion® ionomer dispersion in aliphatic alcohols (Aldrich) and isopropanol solvent (Merck, p.a.) resulting in electrodes with ionomer content of 30% of the total electrode dry mass for the cathode and 40% for the anode [23]. In the case of the trimetallic catalysts Sb_2O_3 salt was added to the ink. The inks were conveniently mixed by stirring with a magnetic stirrer for 30 min followed by sonication with an ultrasonic bath for 15 min. The slurry was painted onto a Nafion 115 (Dupont) membrane with an airbrush (Badger, model 100) and dried in a vacuum oven for 2 hours [23]. The composition of the electrodes regarding the mass of catalysts and metals, measured by weight difference is summarized in Table 1. It should be mentioned that the mass of Sb corresponds to the mass of the oxide salt added into the ink.

Table 1 – Composition of the MEA electrodes.

Catalyst	Cathode	Anode	
	Pt (mg/cm^2)	Pt/PtRu/PtSn (mg/cm^2)	Sb (mg/cm^2)
PtRu/C	2.0	2.1	0
PtRu/C-Sb	2.1	2.6	0.68
Pt/C	1.9	2.3	0
Pt/C - Sb	1.7	2.2	0.7
PtSn/C	2.0	2.1	0

After both the electrodes were painted onto the membrane, the MEA was heat pressed at 130 °C, with 50 kN pressure for 120 s.

The fuel cell experiments were performed in a single cell DAFC with a surface area of 5.29 cm^2 assembled with PTFE gaskets, diffusion layers (carbon cloths, Lodlow Coated products) and the MEA, closed and tightened evenly with 10 kN force. 1 M aqueous solution of ethanol (Altia p.a.) fuel was fed to the anode with 1.5 ml min^{-1} rate and humidified oxygen gas (Aga, 99.999%) to the cathode at 200 ml min^{-1}. The cell was stabilized over night before the measurements with a fuel flow of 0.2 ml min^{-1} and normalized 1 h prior to the polarization experiments with the higher flow rates [23].

For the "in situ" cyclic voltammetry measurements performed in the fuel cell, humidified nitrogen was feed to the anode compartment (serving as a working electrode) to ensure the mass transport through the electrode layer and the membrane. The cathode compartment, used as a reference electrode, was fed with humidified hydrogen flow.

The electrochemical curves were measured with an Autolab PGSTAT 20 instrument equipped with an Autolab BSTR10A booster controlled by GPES software (version 4.9 by Eco Chemie B.V.). The polarization curves were measured with a scan rate of 0.5 mV s^{-1} and the currents obtained are normalized with the cell area.

3. Results and discussion

3.1. Ethanol oxidation on PtRu/C-Sb and its dependence on the Sb coverage

Figure 1 presents the blank voltamograms of Pt/C, Pt/C-Sb, PtRu/C and PtRu/C-Sb with different Sb coverage in 0.5 M H_2SO_4. For Pt/C the blank CV presents two adsorption peaks involving H adsorption at potentials lower that 0.4 V followed by the double layer region at potentials higher than 0.4 V, as expected for the pure Pt catalyst [25]. As for PtRu/C catalysts, the CV (Figure 1A) shows a shorter

potential range (from 0.05 to 0.3 V) for the hydrogen adsorption/desorption in comparison with Pt/C. Following the H adsorption region, there is a region where ruthenium oxides formation begins, increasing the currents in the double layer due to the presence of Ru on the catalyst, as expected [29, 30]. As shown in the CV for Pt/C-Sb in Figure 1A, the irreversible adsorption of Sb onto Pt reduces the number of free Pt sites available for hydrogen adsorption, decreasing consequently the current densities at potentials between 0.06 and 0.4 V (RHE). In the double layer region the presence of Sb can be observed by the appearance of a redox process (0.45 – 0.55 V vs RHE) due to the surface oxidation/reduction of the irreversibly adsorbed Sb, as reported previously [15, 31]. Similar behaviour was observed for PtRu/C catalysts. Adding Sb to PtRu/C (Figure 1 A) leads to the decrease on the currents for H adsorption and, at the same time, to the increase of the currents at higher potentials (overlapping with the Ru surface oxides formation region).

Increasing the stirring time of the ink containing PtRu/C catalyst with Sb salts leads to an increase of the Sb coverage on the catalyst. For the coverages presented in Figure 1B the stirring times are 15, 30 and 45 min for coverages of 0.21, 0.47 and 0.70, respectively. The blank CVs for PtRu/C catalysts with different coverages of Sb are plotted in Figure 1B. Increasing the Sb coverage on the PtRu/C catalyst decreases the currents associated with the H adsorption on Pt due to the blocking of more Pt sites by Sb. At the same time that H adsorption decreases, the currents at high potentials (related with the redox process of Sb [15, 31]) increase. There is a clear dependency on the H region from the Sb coverage, allowing the estimation of the coverage based on the number of Pt sites blocked on the catalyst, as described in the experimental section (Equation 1).

After the electrochemical characterization, ethanol oxidation was studied on the PtRu/C catalysts with different Sb coverages and the correspondent CVs are plotted in Figure 2. As for the blank

voltammograms, for ethanol oxidation the comparison of Pt/C and Pt/C-Sb was also done (Figure 2A). The results show that the addition of Sb to the catalyst substrate, irrespectively whether it is Pt/C or PtRu/C, leads to an increase of its performance for oxidizing ethanol. When comparing Pt and PtRu based catalyst, is possible to observe that those containing Ru show more than 200 mV lower onset potential. In both cases, the addition of Sb does not show any significant increase on the onset potential. For Pt/C catalyst, the presence of Sb shifts the onset potential for the ethanol oxidation to 50 mV lower, however for PtRu/C-Sb the onset is the same than for the unmodified electrode. Nevertheless, the increase of the currents for the modified electrodes is much faster than for the pristine ones. In both cases, the maximum currents at 0.7 V vs RHE are almost doubled in the presence of Sb (0.11 A/mg catalyst for PtRu/C and 0.19 A/mg catalyst for PtRu/C-Sb).

Another interesting result is observed for the PtRu/C-Sb. At currents below 0.4V, the modified catalysts show smaller currents denoting probably higher adsorption of initial ethanol dissociation products [3].

In Figure 2B, the effect of the Sb coverage on the PtRu/C substrate catalysts is shown for ethanol oxidation. The presence of the adatom leads to an increase of the oxidation currents for coverages as high as 0.47 of the full monolayer. For a coverage of 0.7 the currents are, however, lower than for 0.47 suggesting that high surface coverages of Sb are not convenient for ethanol oxidation. The results point out that Sb by itself is not able to catalyze ethanol oxidation and that PtRu sites are needed in order to the reaction take place. In any case, the Sb presence in certain amounts favors the reaction performance, probably taking place in particular ensembles created by the adatom on the PtRu surface, similarly to the effect previously described for Pt/C modified with Sb [15].

The currents obtained from the cyclic voltammetry experiments can be converted using Faraday's law into an approximation of the turnover frequency (TOF) of the catalysts by:

TOF = I normalized/ nF. (Equation 2)

Where I normalized is the current corrected for the n of catalysts on the electrode and for the current efficiency of the system. From our results, the calculation of the correct and precise current efficiency is not possible (because all the methods are qualitative) and the values used for the calculation of the TOF were obtained in the literature for PtRu catalysts [32]. However, as the catalytic activity of PtRu catalysts is strongly dependent on the catalyst composition, the TOF values calculated in this study are only indicative. TOF calculated for ethanol oxidation to CO_2 and to acetic acid at 0.7 and 0.8 V (vs RHE) for the PtRu/C and PtRu/C-Sb catalysts are presented in Table 2.

Table 2 – Values of TOF for CO_2 and acetic acid obtained at 0.7 and 0.8 V (vs RHE) for the studied catalysts.

	TOF (mol of EtOH [mol catalyst]$^{-1}$s^{-1})							
	PtRu/C		**PtRu/C-Sb (0.21)**		**PtRu/C-Sb (0.47)**		**PtRu/C-Sb (0.70)**	
E(V)	**CO_2**	**Acetic Ac.**	**CO_2**	**Acetic Ac.**	**CO_2**	**Acetic Ac.**	**CO_2**	**Acetic Ac.**
0.7	0.010	0.502	0.012	0.618	0.014	0.738	0.011	0.570
0.8	0.014	0.709	0.017	0.890	0.021	1.059	0.017	0.881

The values obtained for the TOF show that, theoretically, the presence of Sb on the PtRu/C catalysts leads to an increase in the values for the conversion of ethanol on both CO_2 and acetic acid. For Sb coverages of 0.47 the TOF for CO_2 and acetic acid are 0.021 and 1.059 mol of ethanol per mol of

catalyst, respectively, the highest values obtained within the studied catalysts. However, the value for acetic acid have a higher increase for medium coverages of Sb (TOF value for acetic acid is almost double for the coverage of 0.47 when compared with PtRu/C). In order to confirm this compounds as products for ethanol oxidation on the modified electrodes and understand the effect of Sb on the catalyst FTIR experiments were also performed and will be presented in the next section.

3.1.1. FTIR experiments

In situ FTIR experiments were performed in order to gain insights in the reaction mechanism for ethanol oxidation on the PtRu/C catalysts modified by Sb. The electrode preparation followed the same procedure as for the electrochemical experiments, but in this case a gold collector was used for the ink deposition. The spectra were obtained in solutions containing 1 M ethanol in 0.1M $HClO_4$ and the 0.1V vs RHE spectrum was taken as a background and subtracted from the spectra recorded at other potentials. 0.1 V was selected as a reference spectrum because at this potential no significant oxidation/adsorption processes should occur [33]. This potential was maintained until the electrode was pressed against the CaF_2 window. After collecting the reference spectrum, the potential was stepped to progressively higher sample potential values, where the corresponding sample spectra were collected (Figure 3). Positive bands correspond to the products formed at the sample potential, during the ethanol oxidation, while negative bands are due to the consumption of species present at the reference potential.

Several bands can be observed in the spectra presented in Figure 3. First, a broad band between 2500 and 3000 cm^{-1} is observed. This band is due to overlapping of the C-H region (2700–3000 cm^{-1}) and the OH from carboxyl group between 2500 and 3000 cm^{-1} and is attributed to the products of incomplete ethanol oxidation (acetic acid and acetaldehyde) [34]. This feature is observed for both the

PtRu/C and PtRu/C-Sb catalysts and becomes more intense with increasing the potential, suggesting higher oxidation rate.

Other observed bands are at 2341 cm^{-1} the C-O asymmetric stretching from CO_2 [34, 35]; at 1710 cm^{-1} the C=O stretching from carbonyl groups either from acetic acid and acetaldehyde [36]; the bands at 1282, 1370–1390 cm^{-1} from C-O stretching and CH_3 bending from acetic acid [36] and, finally a band at 1114 cm^{-1} of CH_3 wagging from acetaldehyde [37] that overlaps with ClO_4^- band from the supporting electrolyte

It is important to notice that any of the spectra presented in Figure 3 shows bands related to CO on the surfaces in the potential range studied. This fact cannot be taken as an indication that CO is absent under these conditions but more likely that the CO oxidation at these potentials is faster than its production and the corresponding IR bands stay below the detection limit. Moreover, it is well known that on Pt nanoparticles the CO oxidation to CO_2 is expected to be fast due to the small size of the sites and because the surface is formed in majority by defects and steps [38].

All the identified bands are observed for both of the catalyst suggesting that the presence of Sb does not have a pronounced effect on the reaction mechanism, or at least the final products of the reaction are identical for the two catalysts. However, the relative intensity of the bands changes with the catalyst. For easier interpretation the integration of the bands due to acetaldehyde (1140 cm^{-1}), acetic acid (1280 cm^{-1}), CO_2 (2341 cm^{-1}) and the ration between the bands at 1710 (acetaldehyde and acetic acid) and 1282 cm^{-1} (acetic acid) is presented in Figure 4.

The first result that these plots highlights is that significant amounts of acetaldehyde are observed for lower potentials in PtRu/C-Sb catalyst, although the onset potentials are identical with both catalysts. Even at potentials lower than the onset potential for the oxidation reaction observed in the CV, the

acetaldehyde band is more intense for PtRu/C-Sb than for PtRu/C. It has been reported earlier [39], that acetaldehyde is a possible intermediate on the C-C bond breaking from ethanol at potentials as low as 0.1 V.

However, the band from acetaldehyde (at 1114 cm^{-1}) occurs in the same region than ClO_4^- present in the system due to the supporting electrolyte composition. When the electrode potential is increased we should have migration of the negative species (ClO_4^-) to the thin layer which will also result in an increase of the band at ~1100 cm^{-1}. Knowing that the perchlorate concentration is the same in both the experiments (for PtRu/C and PtRu/C-Sb) its influence on the band intensity should be very similar on both the catalysts and the differences can be interpreted as consequence of the different amounts of acetaldehyde produced on the catalyst. Another way to compare the relative amounts of acetaldehyde and acetic acid [36] is to look into the ration of the bands at 1710 and 1282 cm^{-1} (the first band have contributions from acetaldehyde and the other from acetic acid). The plot of this ration is show in panel D of Figure 4 and, as it is possible to observe, the lower value for the ration for PtRu/C-Sb suggested higher formation of acetic acid than acetaldehyde for potentials higher than 0.3 V (vs RHE).

These results, together with the higher band for CO_2 in the trimetallic catalysts at 0.6 V (Figure 4), suggest that the dissociation of ethanol though the C-C bond breaking with acetaldehyde as an intermediate is favored on PtRu/C-Sb catalyst. Yet, at higher potentials (>0.5V) the intensity of the IR band for acetaldehyde decreases (as well as the ration between the bands at 1710 and 1282 cm^{-1}) for PtRu/C-Sb when compared with PtRu/C, at the same time that the acetic acid band increases rapidly. Most likely, on the modified electrode acetaldehyde is being oxidized further to acetic acid which can be considered as the major product of ethanol oxidation on the modified catalyst.

On the PtRu/C catalyst, the main reaction product is acetaldehyde, although acetic acid and CO_2 are also observed. Both acetic acid and acetaldehyde formation are observed at the same potential range, but acetaldehyde formation is favored at higher potentials (as observed also with the decrease on the ration between the bands at 1710 and 1282 cm^{-1}) at the same time that CO_2 formation is observed.

As mentioned previously, it is assumed that Ru acts as an oxygen supplier at low potentials, diminishing the poisoning effect from the adsorbed intermediates. This effect is clearly observed when the cyclic voltammetry results obtained for Pt and PtRu catalysts are compared (Figure 2). However, the addition of another oxophilic metal can still result in an improvement of the catalytic activities toward ethanol oxidation reactions [9, 12, 13]. For Sb adsorbed onto pure Pt catalysts it has been shown that Sb favours a bifunctional mechanism through an adatom-meditated oxygen transfer, where Sb provides oxygenated species at low potentials favouring ethanol and CO oxidation at earlier stage [15]. For the trimetallic catalyst (PtRu/C-Sb) studied here, the enhancement of the catalytic activity is probably caused by a synergetic effect between Ru as oxygen supplier and Sb whose oxophilicity enhances the water oxidation, leading to the early formation of adsorbed hydroxides acting as oxidants for the strongly adsorbed intermediates as acetaldehyde. However, the direct oxidation to CO_2 is not the main reaction path on these trimetallic surfaces.

3.2. Fuel Cell experiments

The catalysts previously characterized by electrochemical and spectroelectrochemical experiments were tested under real fuel cell conditions. To ensure the presence of Sb in the modified electrode in situ cyclic voltammetry was performed and the results are shown in Figure 5. Cyclic voltammetry from

the anode electrodes allows following any change on the catalyst amount or in the adatom coverages during the fuel cell experiments.

The CVs resemble those described in the previous section (see Figure 1) devoted to the electrochemical characterization. The presence of Sb is revealed by the decrease in the H adsorption region and the increase in the currents at aprox. 0.5 V due to the redox process of Sb. The absence of clearly defined features for H adsorption or for Sb oxidation process in these CVs is due to the experimental configuration used. The voltammetry is obtained using the anode of the Membrane Electrode Assembly (MEA) containing ionomer as working electrode and the Nafion membrane as an electrolyte.

The polarization curves obtained from the direct ethanol fuel cell with the PtRu/C and PtRu/C-Sb anode catalysts are presented in Figure 6 A. The respective power curves calculated from the cell voltage and resulting current for the same catalysts are also presented in Figure 6 B.

The results show that, as expected from the electrochemical results, the presence of Sb leads to higher current densities at lower cell potentials and, consequently to higher power densities. The open circuit voltage (OCV) increases due to the addition of small amounts of Sb (from 0.70 for PtRu/C to 0.74 with PtRu/C-Sb) as already suggested from the electrochemical behaviour of the same catalyst. However, the decreasing of poisoning at the anode surface is noticeable by the increase on the current densities already from a high cell potential of 0.6 V. For example, at 0.3 V the current for PtRu/C is 34.28 mA/cm^2 while for PtRu/C-Sb the value reached is 68.06 mA/cm^2. The maximum power densities obtained with these catalysts are 12.10 and 23.27 mW/cm^2 for PtRu/C and PtRu/C-Sb, respectively. These values are both significantly higher than those obtained under the same fuel cell conditions for pure Pt [23]. However, with the trimetallic catalyst a power density 2 times higher than that with PtRu/C still achieved. The maximum power per mg of Pt is 13.44 mW and it is in the same range than

reported for other trimetallic catalysts [17-20] obtained by more complicated and expensive synthesis methods (Table 3).

Table 3 – Comparison of the open circuit potentials, maximum power density of the catalysts and values in the literature for PtRu based catalysts.

Catalyst	Temperature (^{0}C)	OCV (V)	Maximum Power density (mW/cm^2)	Reference
PtRu/C	70	0.70	12.10	This work
PtRu/C-Sb		0.74	23.27	
PtRuSn	88	0.655	24.2	[17]
PtRuSn		0.686	27.5	
PtRuSn		0.655	27.5	
PtRu/C	90	0.677	28.54	[9]
PtRuW/C		0.698	38.54	
PtRuMo/C		0.720	31.19	
PtRu/C	90	0.69	12	[40]
PtRuIrSn		0.700	15	

In order to check the stability of this modified PtRu/C-Sb catalysts, chronoamperometric curves were obtained at the cell potential of 0.3 V during 1 h at 70º C. The results obtained for PtRu/C and PtRu/C-Sb are plotted in Figure 7. As expected from the previously presented results, higher current densities are obtained for PtRu/C-Sb. Moreover, the deactivation of the catalysts seems to be less pronounced once the decrease in the currents with time is smaller than in the bimetallic catalyst. These results show

that, in addition to the better performances, the modified catalysts are also more stable under fuel cell working conditions.

As observed in Table 3, the direct comparison of fuel cell results reported by different groups requires some careful standardization once that relevant experimental conditions can vary from one group to the other and those will have a big influence on the cells performances. For example, comparison between results obtained at 70 or 90 ^{0} C or with and without back pressure in the oxidant flow is very problematic. For this reason, the power curves obtained for PtRu/C, PtRu/C-Sb, Pt/C, Pt/C-Sb and PtSn/C in the same fuel cell conditions are presented in Figure 8.

In agreement with previous reports [23], the presence of Sb clearly increases the fuel cell performance either as a bimetallic (Pt/C-Sb) or trimetallic (PtRu/C-Sb) catalysts. The improvement surpasses the performances obtained for PtSn/C catalysts, which have been described as the best bimetallic catalyst for the DEFC. The OCV and the maximum power densities for the PtRu/C-Sb catalyst is the highest within the catalyst presented in this study. A summary of the general performance of the catalysts plotted in Figure 7 is presented in Table 4.

Table 44 – Open circuit potentials, maximum power density, normalized maximum power density and normalized current at 0.1V (Ecell) for all the catalysts from Figure 8, at 70°C.

Catalyst	OCV (V)	Maximum Power density (mW/cm^2)	Normalized maximum power (W/g Pt)	Normalized currents @ 0.1V ($mA/\mu g_{pt}$)
PtRu/C	0.70	12.10	9.60	0.690
PtRu/C-Sb	0.74	23.27	14.92	1.010
Pt/C	0.34	3.33	1.44	0.029
Pt/C-Sb	0.52	15.26	6.94	0.055

PtSn/C	0.67	11.70	11.14	0.740

Appropriated physical characterization of the MEA's and catalyst (XRD, SEM, etc.) were performed and are included as supporting material. As a summary these results show that there is no evidence of effects of Sb on the structure of the MEA, catalyst lattice constants and particles size that can justify the better performance of the catalyst. Based on this information and on the obtained results we can suggest that the increase in the performance of the PtRu/C catalyst after addition of Sb, observed both in an electrochemical and in fuel cell conditions, is due to the decrease of the surface poisoning by adsorbed species because Sb oxophilicity enhances water oxidation, leading to the early formation of adsorbed hydroxides acting as oxidants for those strongly adsorbed intermediates. The lower degree of adsorption of the intermediates, as acetaldehyde, can cause its earlier oxidation to acetic acid increasing the overall fuel cell performance.

4. Conclusions

In this paper we report the performance of PtRu/C-Sb as a catalyst for ethanol oxidation and as an anode electrode in a direct ethanol fuel cell. This trimetallic catalyst is easily prepared just by adding a Sb salt to the ink of the PtRu/C catalyst commercially available. By the presence of Sb on PtRu an increase on its catalytic activity for ethanol oxidation reaction was observed. The catalytic effect revealed to be dependent on the Sb coverage and increasing oxidation currents were obtained for increasing coverages till 0.47. For coverage higher than 0.47 the activity starts to decrease showing that

PtRu free sites are requires for the catalytic effect and that Sb is no active by itself. FTIR experiments show that the mechanism of the reaction is not significantly changed by the foreigner metal but the main reaction product is acetic acid. No higher formation of CO_2 was found.

In the fuel cell, the increase in the catalytic properties of the trimetallic anode is revealed by the increase of the currents and power densities obtained in the direct ethanol fuel cell measurements. The presence of Sb on the catalyst duplicated the power densities and the fuel cell performance obtained when compared with PtRu/C. In comparison with other catalyst anodes (Pt/C, Pt/C-Sb and PtSn/C), PtRu/C-Sb presents the highest currents and power densities. The enhancement of the catalytic behaviour and the fuel cell performance can be explained by the synergy between the effects of Ru, as oxygen supplier and Sb that due to its oxophilicity enhances the water oxidation, leading to the early formation of adsorbed hydroxides which act as oxidants for the strongly adsorbed intermediates. In addition to the better performances, the modified catalyst is also more stable under fuel cell conditions.

Acknowledgements

The financial support from Aalto University is acknowledged. This work made use of the Aalto University Nanomicroscopy Center (Aalto-NMC) premises. JMF and R.M.A.A would like to thank MICINN through project CTQ2013-44083-P.

References

[1] M.Z.F. Kamarudin, S.K. Kamarudin, M.S. Masdar, W.R.W. Daud, International Journal of Hydrogen Energy, 38 (2013) 9438-9453.
[2] H. Hitmi, E.M. Belgsir, J.M. Léger, C. Lamy, R.O. Lezna, Electrochimica Acta, 39 (1994) 407-415.
[3] T. Iwasita, E. Pastor, Electrochimica Acta, 39 (1994) 531-537.

[4] J.F. Gomes, K. Bergamaski, M.F.S. Pinto, P.B. Miranda, Journal of Catalysis, 302 (2013) 67-82.
[5] E. Antolini, Journal of Power Sources, 170 (2007) 1-12.
[6] S.S.D. Gupta, Jayati, Journal of Chemical Sciences, 117 (2005) 337-344.
[7] A. Rabis, P. Rodriguez, T.J. Schmidt, ACS Catalysis, 2 (2012) 864-890.
[8] F. Vigier, C. Coutanceau, F. Hahn, E.M. Belgsir, C. Lamy, Journal of Electroanalytical Chemistry, 563 (2004) 81-89.
[9] W. Zhou, Z. Zhou, S. Song, W. Li, G. Sun, P. Tsiakaras, Q. Xin, Applied Catalysis B: Environmental, 46 (2003) 273-285.
[10] T.S. Almeida, L.M. Palma, P.H. Leonello, C. Morais, K.B. Kokoh, A.R. De Andrade, Journal of Power Sources, 215 (2012) 53-62.
[11] S.C. Zignani, V. Baglio, J.J. Linares, G. Monforte, E.R. Gonzalez, A.S. Aricò, International Journal of Hydrogen Energy, 38 (2013) 11576-11582.
[12] F. Colmati, E. Antolini, E.R. Gonzalez, Journal of Power Sources, 157 (2006) 98-103.
[13] N. Fujiwara, K.A. Friedrich, U. Stimming, Journal of Electroanalytical Chemistry, 472 (1999) 120-125.
[14] M.M. Tusi, N.S.O. Polanco, S.G. da Silva, E.V. Spinacé, A.O. Neto, Electrochemistry Communications, 13 (2011) 143-146.
[15] M.C. Figueiredo, A. Santasalo-Aarnio, F.J. Vidal-Iglesias, J. Solla-Gullón, J.M. Feliu, K. Kontturi, T. Kallio, Applied Catalysis B: Environmental, 140–141 (2013) 378-385.
[16] A. Brouzgou, S.Q. Song, P. Tsiakaras, Applied Catalysis B: Environmental, 127 (2012) 371-388.
[17] Y.H. Chu, Y.G. Shul, International Journal of Hydrogen Energy, 35 (2010) 11261-11270.
[18] M. Li, A. Kowal, K. Sasaki, N. Marinkovic, D. Su, E. Korach, P. Liu, R.R. Adzic, Electrochimica Acta, 55 (2010) 4331-4338.
[19] X.-H. Jian, D.-S. Tsai, W.-H. Chung, Y.-S. Huang, F.-J. Liu, Journal of Materials Chemistry, 19 (2009) 1601-1607.
[20] G. García, N. Tsiouvaras, E. Pastor, M.A. Peña, J.L.G. Fierro, M.V. Martínez-Huerta, International Journal of Hydrogen Energy, 37 (2012) 7131-7140.
[21] Z.-B. Wang, G.-P. Yin, Y.-G. Lin, Journal of Power Sources, 170 (2007) 242-250.
[22] E. Lee, A. Murthy, A. Manthiram, Electrochimica Acta, 56 (2011) 1611-1618.
[23] M.C. Figueiredo, O. Sorsa, N. Doan, E. Pohjalainen, H. Hildebrand, P. Schmuki, B.P. Wilson, T. Kallio, Journal of Power Sources, 275 (2015) 341-350.
[24] G.A. Camara, R.B. de Lima, T. Iwasita, Electrochemistry Communications, 6 (2004) 812-815.
[25] A. López-Cudero, J. Solla-Gullón, E. Herrero, A. Aldaz, J.M. Feliu, Journal of Electroanalytical Chemistry, 644 (2010) 117-126.
[26] M. Figueiredo, V. Climent, J. Feliu, Electrocatal, 2 (2011) 255-262.
[27] A.M. Gómez-Marín, A. Berná, J.M. Feliu, The Journal of Physical Chemistry C, 114 (2010) 20130-20140.
[28] N.M. Cantillo, J. Solla-Gullón, E. Herrero, C. Sánchez, ECS Transactions, 41 (2011) 1307-1316.
[29] S.L. Gojković, T.R. Vidaković, D.R. Đurović, Electrochimica Acta, 48 (2003) 3607-3614.
[30] A. Santasalo-Aarnio, E. Sairanen, R.M. Arán-Ais, M.C. Figueiredo, J. Hua, J.M. Feliu, J. Lehtonen, R. Karinen, T. Kallio, Journal of Catalysis, 309 (2014) 38-48.
[31] V. Climent, N. García-Aráez, J.M. Feliu, Clues for the Molecular-Level Understanding of Electrocatalysis on Single-Crystal Platinum Surfaces Modified by p-Block Adatoms, in: Fuel Cell Catalysis, John Wiley & Sons, Inc., 2008, pp. 209-244.
[32] H. Wang, Z. Jusys, R.J. Behm, Journal of Power Sources, 154 (2006) 351-359.
[33] S.C.S. Lai, M.T.M. Koper, Faraday Discussions, 140 (2009) 399-416.
[34] X.H. Xia, H.D. Liess, T. Iwasita, Journal of Electroanalytical Chemistry, 437 (1997) 233-240.
[35] T. Iwasita, B. Rasch, E. Cattaneo, W. Vielstich, Electrochimica Acta, 34 (1989) 1073-1079.

[36] F. Colmati, G. Tremiliosi-Filho, E.R. Gonzalez, A. Berna, E. Herrero, J.M. Feliu, Faraday Discussions, 140 (2009) 379-397.
[37] V. Del Colle, A. Berna, G. Tremiliosi-Filho, E. Herrero, J.M. Feliu, Physical Chemistry Chemical Physics, 10 (2008) 3766-3773.
[38] Q.-S. Chen, J. Solla-Gullón, S.-G. Sun, J.M. Feliu, Electrochimica Acta, 55 (2010) 7982-7994.
[39] S.C.S. Lai, S.E.F. Kleyn, V. Rosca, M.T.M. Koper, The Journal of Physical Chemistry C, 112 (2008) 19080-19087.
[40] K. Fatih, V. Neburchilov, V. Alzate, R. Neagu, H. Wang, Journal of Power Sources, 195 (2010) 7168-7175.

Figure 1 – Blank CV for A) comparison between Pt/C, Pt/C-Sb, PtRu/C and PtRu/C-Sb catalysts and B) PtRu/C catalysts with increasing Sb coverages. CV obtained in 0.5 M H_2SO_4, 50 mV/s with 0.02 mg/cm^2 of catalyst.

Figure 2 – CVs for ethanol oxidation A) on Pt/C, Pt/C-Sb, PtRu/C and PtRu/-Sb and B) effect of the Sb coverage over PtRu/C. CVs obtained for 1M ethanol in 0.1 M $HClO_4$ at 50mV/s with 0.02 mg/cm^2 of catalyst.

Figure 3 – FTIR spectra obtained ethanol oxidation (1M in 0.1M $HClO_4$) at PtRu/C and PtRu/C –Sb (θ = 0.34). Reference potential: 0.1V vs RHE, 100 scans at 8 cm^{-1} resolution.

Figure 4 - Integration of the bands at 1280 (acetic acid), 1114 (acetaldehyde), 2341 cm^{-1} (carbon dioxide) and the ration between the bands 1710 (acetaldehyde and acetic acid) and 1282 cm^{-1} (acetic acid) for PtRu/C and PtRu/C–Sb (θ = 0.34).

Figure 5 – CVs obtained under fuel cell condition for PtRu/C and PtRu/C-Sb anodes. Cathode: 2.0 ± 0.2 mg of Pt/C; Anode: 2.32 ± 0.3 mg of PtRu/C.

Figure 6 – A) Polarization and B) power curves obtained for PtRu/C and PtRu/C-Sb anode catalyst in a direct ethanol fuel cell at 70°C. Fuel: 1M ethanol; Oxidant: 200mL/min of O_2. Cathode: 2.0 ± 0.2 mg of Pt/C; Anode: 2.32 ± 0.3 mg of PtRu/C.

Figure 7 – Chonoamperometric curves for PtRu/C and PtRu/C-Sb anodes at 0.3 V in a DEFC.
Cathode: 2.0 ± 0.2 mg of Pt/C; Anode: 2.32 ± 0.3 mg of PtRu/C.

Figure 8 – Power curves obtained for PtRu/C, PtRu/C-Sb, Pt/C, Pt/C-Sb and PtSn/C at 70^0 C, 1 M ethanol and 200ml/min oxygen flow. Cathode: 2.0 ± 0.2 mg of Pt/C; Anode: 2.3 ± 0.3 mg of catalyst.

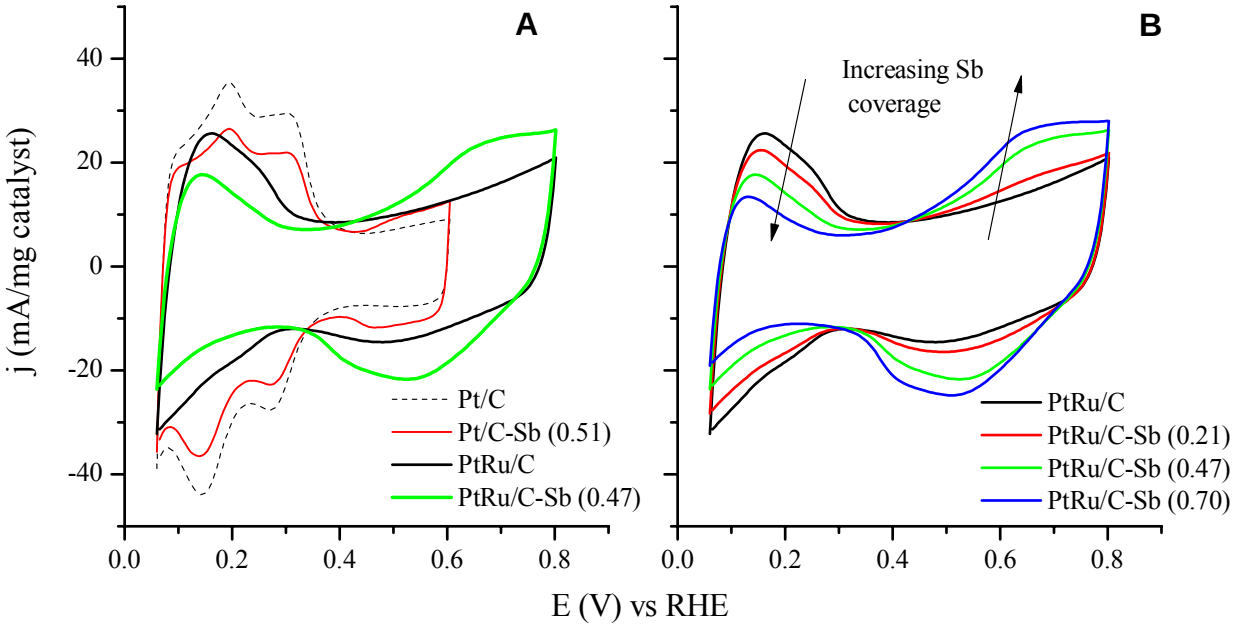

Figure 1 – Blank CV for A) comparison between Pt/C, Pt/C-Sb, PtRu/C and PtRu/C-Sb catalysts and B) PtRu/C catalysts with increasing Sb coverages. CV obtained in 0.5 M H_2SO_4, 50 mV/s with 0.02 mg/cm^2 of catalyst.

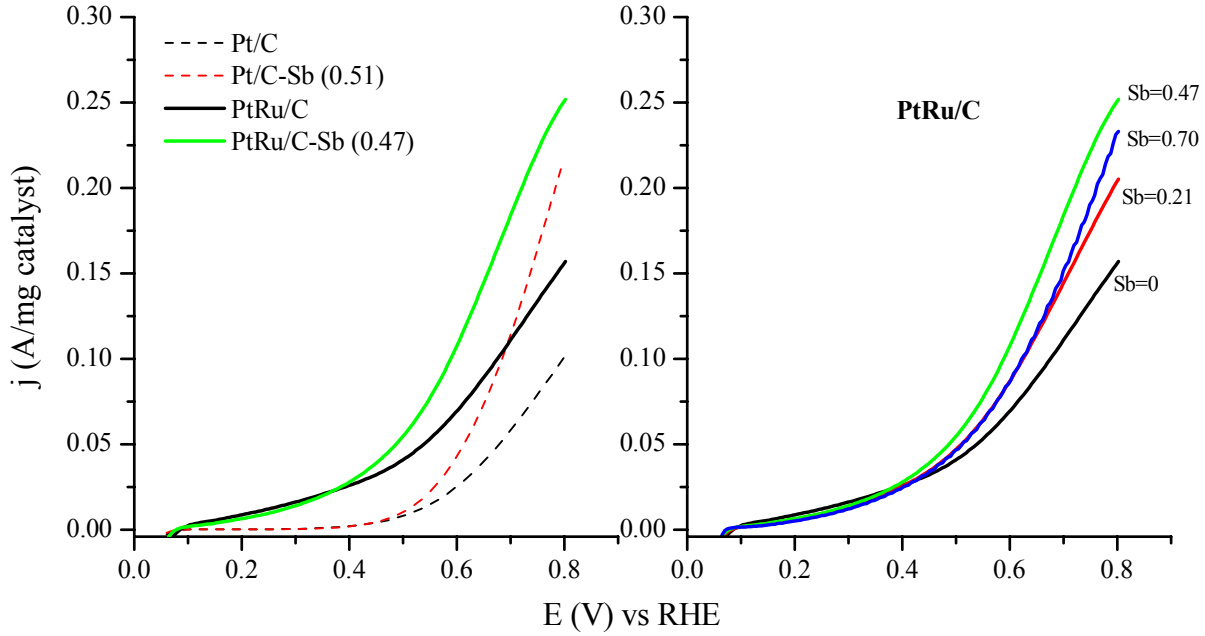

Figure 2 – CVs for ethanol oxidation A) on Pt/C, Pt/C-Sb, PtRu/C and PtRu/-Sb and B) effect of the Sb coverage over PtRu/C. CVs obtained for 1M ethanol in 0.1 M $HClO_4$ at 50mV/s with 0.02 mg/cm^2 of catalyst.

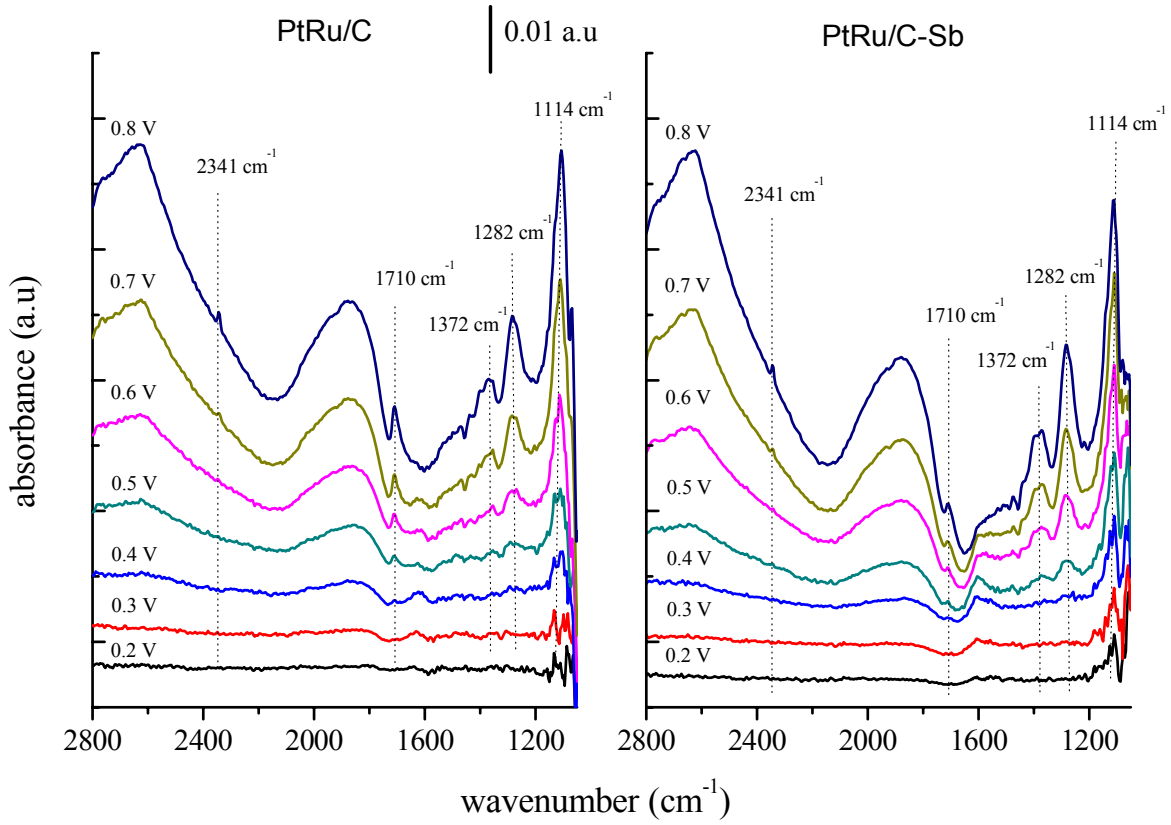

Figure 3 – FTIR spectra obtained ethanol oxidation (1M in 0.1M $HClO_4$) at PtRu/C and PtRu/C –Sb (θ = 0.34). Reference potential: 0.1V vs RHE, 100 scans at 8 cm^{-1} resolution.

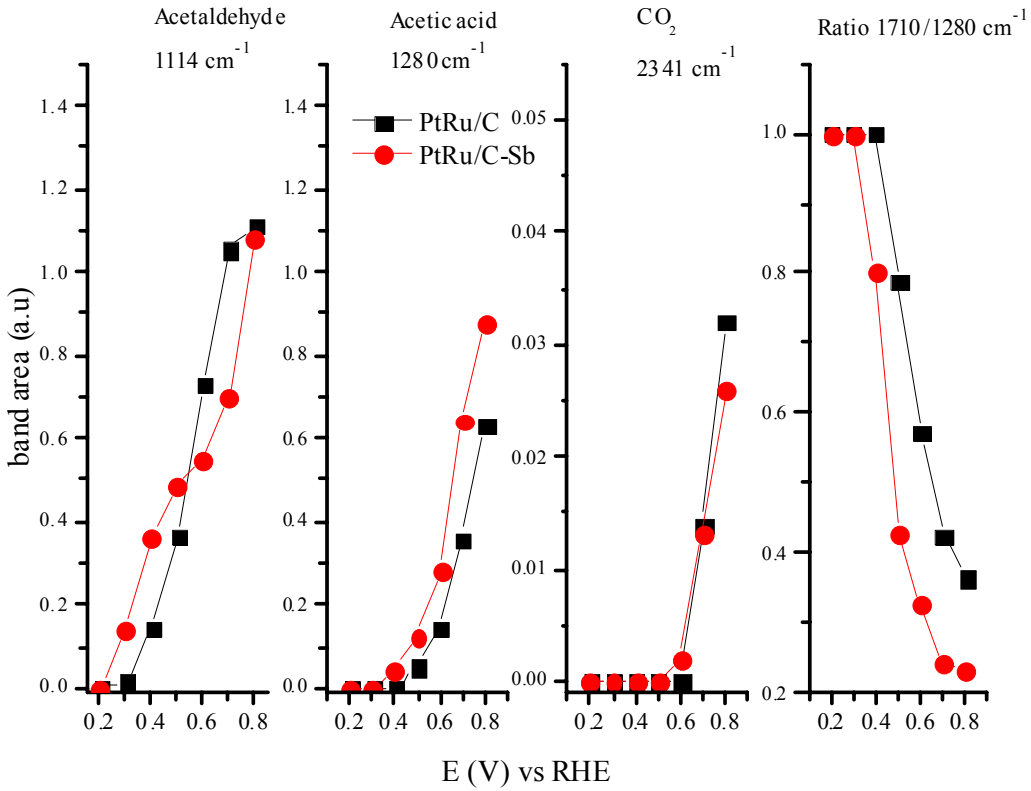

Figure 4 - Integration of the bands at 1280 (acetic acid), 1114 (acetaldehyde), 2341 cm^{-1} (carbon dioxide) and the ration between the bands 1710 (acetaldehyde and acetic acid) and 1282 cm^{-1} (acetic acid) for PtRu/C and PtRu/C–Sb (θ = 0.34).

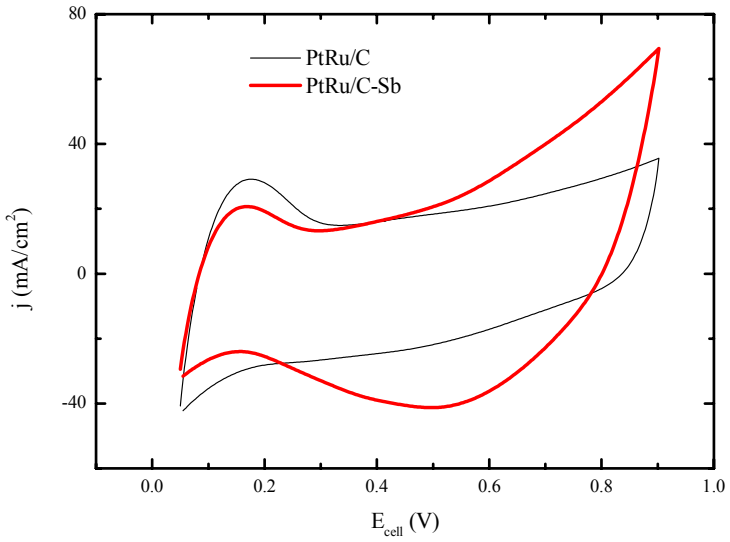

Figure 5 – CVs obtained under fuel cell condition for PtRu/C and PtRu/C-Sb anodes. Cathode: 2.0 ± 0.2 mg of Pt/C; Anode: 2.32 ± 0.3 mg of PtRu/C.

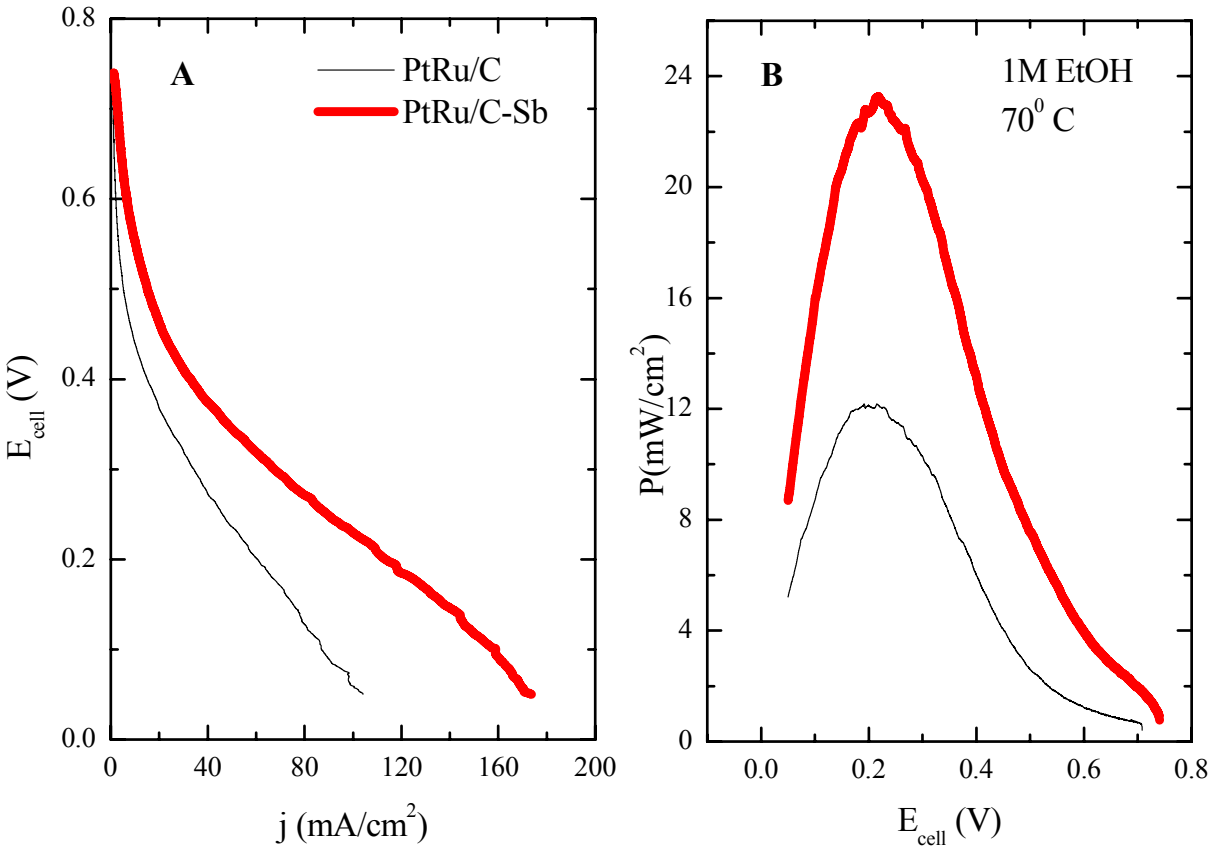

Figure 6 – A) Polarization and B) power curves obtained for PtRu/C and PtRu/C-Sb anode catalyst in a direct ethanol fuel cell at 70°C. Fuel: 1M ethanol; Oxidant: 200mL/min of O_2. Cathode: 2.0 ± 0.2 mg of Pt/C; Anode: 2.32 ± 0.3 mg of PtRu/C.

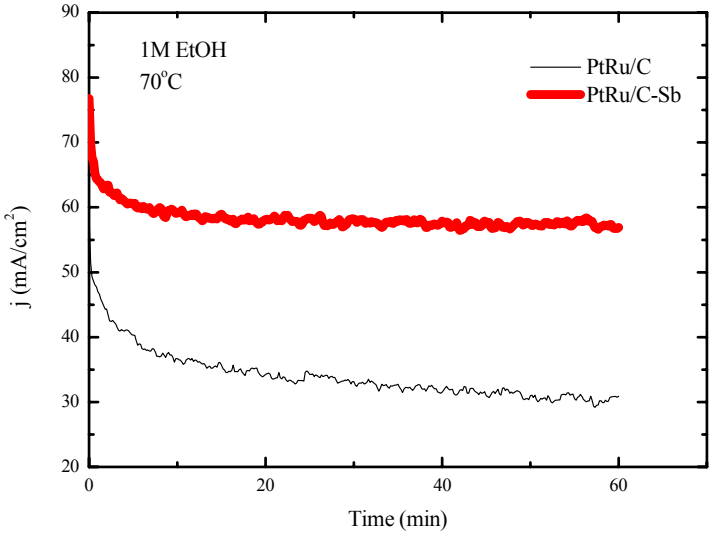

Figure7 – Chonoamperometric curves for PtRu/C and PtRu/C-Sb anodes at 0.3 V in a DEFC. Cathode: 2.0 ± 0.2 mg of Pt/C; Anode: 2.32 ± 0.3 mg of PtRu/C.

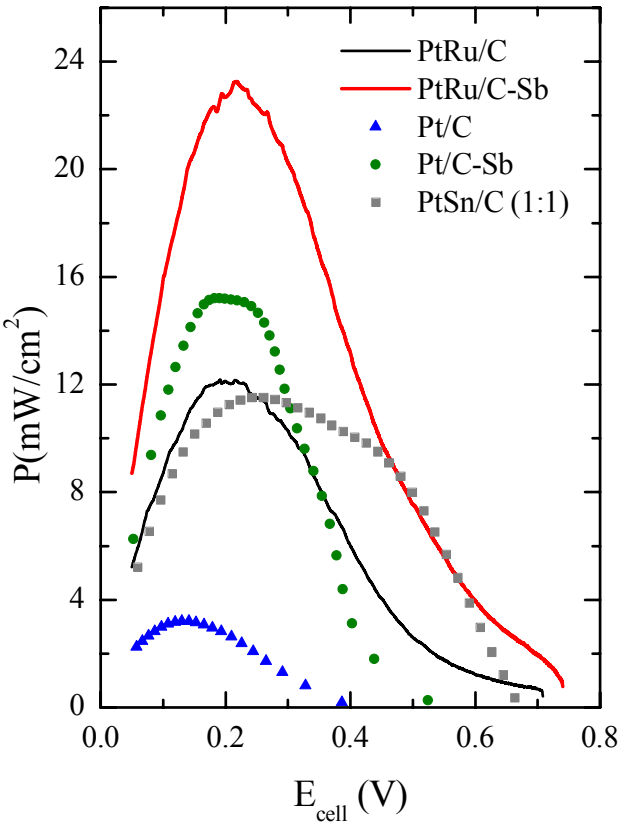

Figure 8 – Power curves obtained for PtRu/C, PtRu/C-Sb, Pt/C, Pt/C-Sb and PtSn/C at 70^0 C, 1 M ethanol and 200ml/min oxygen flow. Cathode: 2.0 ± 0.2 mg of Pt/C; Anode: 2.32 ± 0.3 mg of catalyst.

Supporting Information

Tri-metallic catalyst based on PtRu modified by irreversible adsorption of Sb for direct ethanol fuel cells

Marta C. Figueiredo[1,a] , Olli Sorsa1, Rosa M. Arán-Ais[2], Nguyet Doan[1], Juan M. Feliu[2], Tanja Kallio[1]

[1] Research group of Fuel Cells, School of Chemical Technology, Aalto University, P.O. Box 16100, 00076 Aalto, Finland

[2] Instituto de Electroquímica, Universidad de Alicante, Ap. 99, E-03080, Alicante, Spain.

Sb adsorption on Ru/C

Figure 1 shows the comparison between the blank CVs obtained for Ru/C and GC electrodes pristine and after modification with Sb with the CVs obtained for these surfaces on the presence of ethanol.

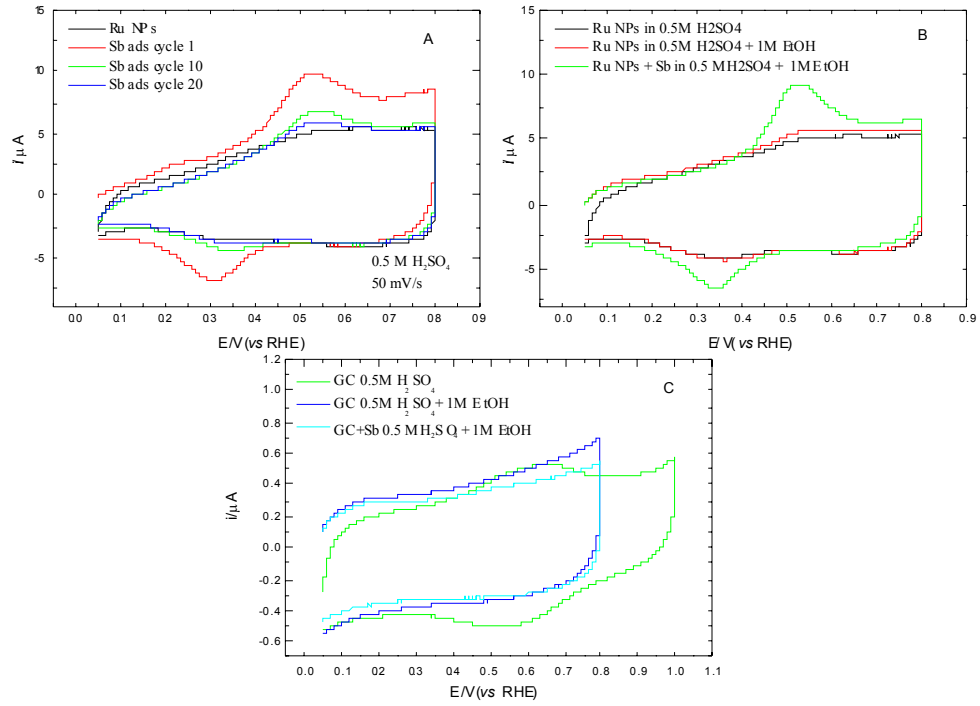

Figure S1 – CVs obtained for Ru/C and Ru/C-Sb catalyst A) in 0.5 M H_2SO_4, B) in 1M EtOH in 0.5 M H_2SO_4 and C) CVs for a glassy carbon electrode (GC) in 0.1 M EtOH and 0.5M H_2SO_4 pure and for GC modified with Sb.

Catalyst layer characterization

Once fuel cell measurements were performed, scanning electron microscopy (SEM) images from the surface of the anode were taken, using a JEOL JSM-7500FA field emission scanning electron microscope equipped with an energy-dispersive X-ray spectrometer (EDXS). The EDXS spectra were used to investigate the elemental analysis of the catalyst as well as to perform a mapping of the metals distribution on the carbon. All of the studied catalysts were characterized by X-ray diffraction (XRD)

(PanAnalytical X'Pert Pro). The XRD diffractograms were used to calculate the size of crystalline domains using the Scherrer equation (Equation 2):

$$d = \frac{0.9\lambda}{\beta_{2\theta}\cos\theta} \qquad \text{(Equation 2)}$$

where d is the average crystalline domain diameter in nm, λ is the X-ray wavelength (Cu target 1.540Å), θ is the Bragg angle in radians, and $\beta_{2\theta}$ is the full width at half maximum (FWHM) in radians.

The SEM images are presented in Figure S1 and it can be observed that the addition of Sb to the catalysts does not have any influence on the anode layer structure. Even after Sb adsorption the porous structure of the catalyst is maintained.

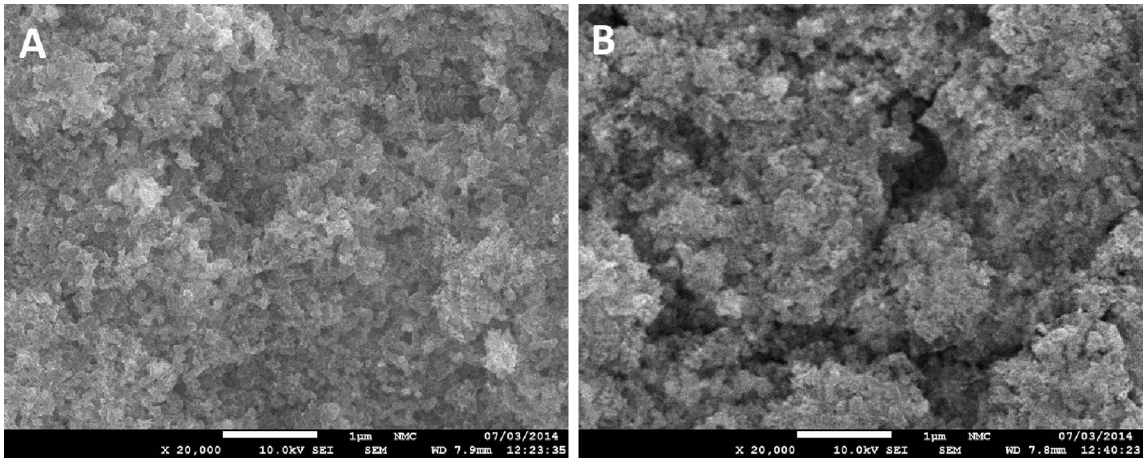

Figure S2 – SEM images from the anode catalyst layers: A) PtRu/C and B) PtRu/C-Sb.

The EDXS spectrum obtained for the PtRu/C-Sb anode catalyst is presented in Figure S2.

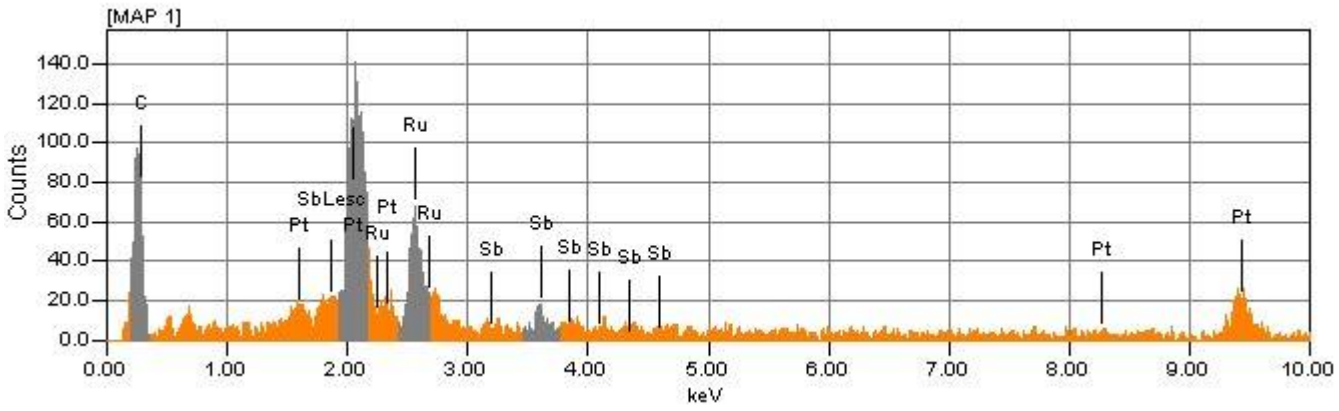

Figure S3 – EDXS spectrum of PtRu/C-Sb anode.

Table S1 – Composition of the anode layers obtained from the EDXS spectrum of PtRu/C-Sb.

Element	wt%	mol%
C	39.14	88.74
Ru	17.26	4.65
Sb	6.2	1.39
Pt	37.4	5.22
Total	100	100

The mapping of the metals on the anode surface is shown in Figure S3 and Table S1. The results show a very good distribution of Sb over the analyzed surface area of the anode revealing the great validity of this simple method for catalyst preparation.

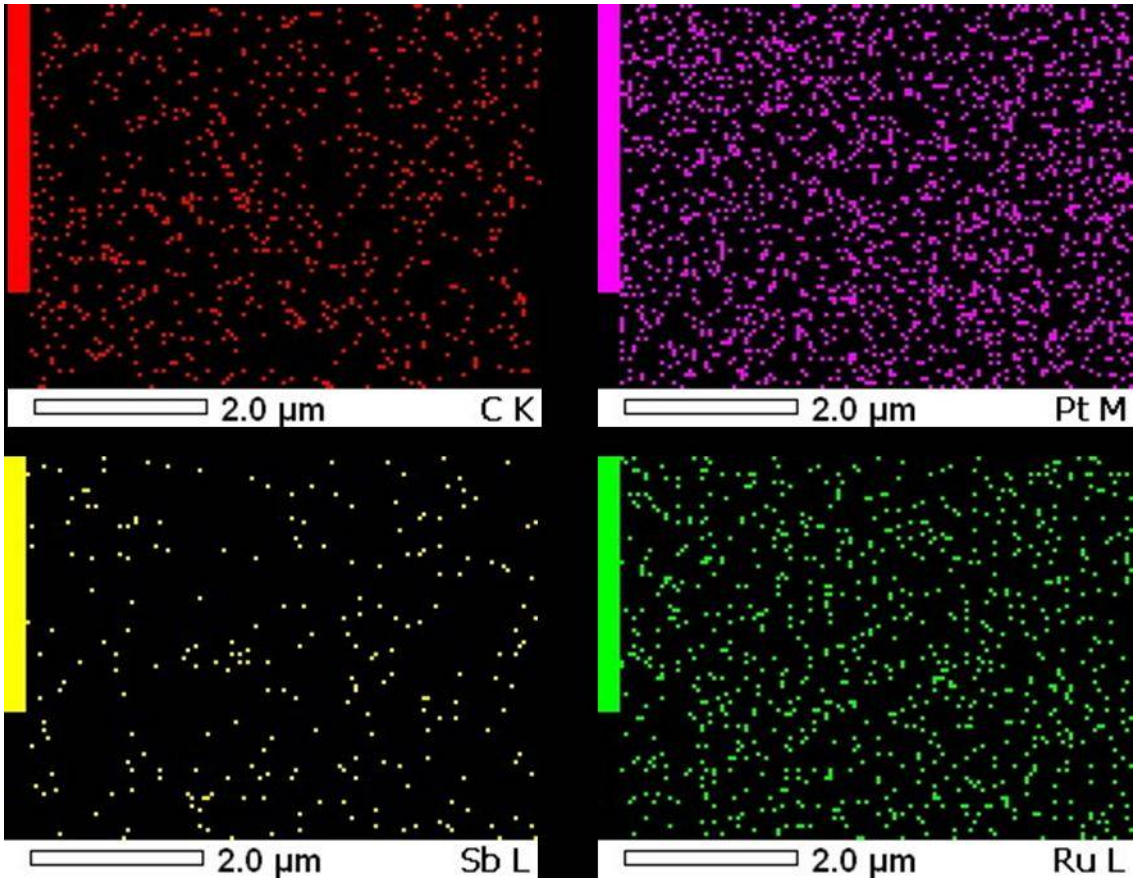

Figure S4 – EDXS mapping from the anode prepared by irreversible adsorption of Sb onto PtRu/C.

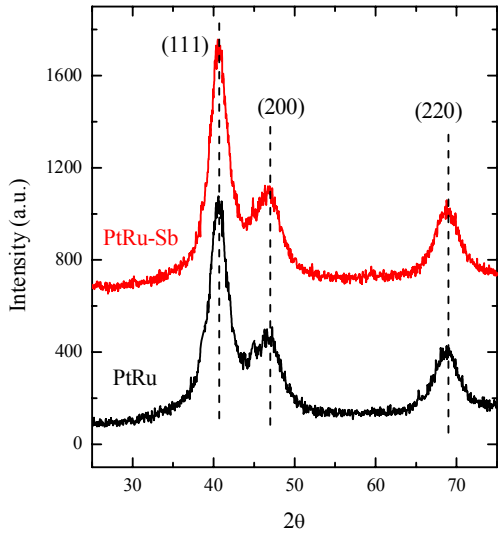

Figure S52 – XRD spectra for PtRu/C and PtRu/C-Sb.

XRD measurements were performed to study the crystal structure of the catalysts. The XRD diffractograms of all the catalysts show wide peaks, indicating the small size of the particles. Four main peaks were observed in all the samples assigned to a face-centered-cubic (fcc) crystal phase (Figure S4). More detailed analysis shows peaks at 2θ positions — 39.6°, 45.7°, 67.6°, and 81.5°—indicating a metallic Pt corresponding to (1 1 1), (2 0 0), (2 2 0), and (3 1 1) planes [35] (JCPDS card 01-087-0647), respectively (Figure S3). The particle sizes calculated on the basis of the XRD results are presented in Table S2.

Table 2 – particles size and lattice parameters obtained from the XRD data.

Catalyst	D (nm)	a (lattice parameter)
PtRu/C	2.27	3.88
PtRu/C-Sb	2.63	3.85

No significant differences are found on the catalyst structure after Sb depositions. The addition of Sb did not cause any shift on the position of the Pt peaks suggesting that PtRu and Sb do not form any alloy and that Sb is probably confined to the metal particles surface. No evidences of metallic Ru and Sb (or any oxide phase) were found. However, based on previous reports for Pt based catalysts modified with Bi and Sb the presence of oxide forms cannot be ruled out[1].

PtSn nanoparticles synthesis

Platinum-tin (PtSn) nanoparticles were synthetized by reduction of mixtures of H_2PtCl_6 and $SnCl_2$ (Sigma Aldrich) with sodium borohydride (NaBH4, Merck) using a water in oil microemulsion of water/polyethylenglycol-dodecylether (BRIJ®30, Aldrich)/*n*-

heptane (Merck) [2]. The synthesis was achieved by preparing a microemulsion containing the aqueous solution of the metallic precursors (Pt, Sn) and a fixed amount of water to surfactant molar ratio (ω_0=3.8) and same surfactant concentration. The amount of surfactant, in volume, amounts to 16.5% of the total volume of the microemulsion. The concentrations of H_2PtCl_6 and $SnCl_2$ were 0.1 M, and the amount of $NaBH_4$ was in stoichiometric excess. For the preparation of PtSn, an aqueous solution of H_2PtCl_6+ $SnCl_2$ with a convenient atomic proportion of the two elements was employed. After the complete reduction of the precursors, Vulcan Carbon® XC-72 was added as a support for nanoparticles to a nominal loading of 20 % of metal in the electrocatalysts. When the synthesis was done, the supported nanoparticles were conveniently washed with acetone to cause phase separations and methanol to eliminate surfactant molecules. Finally, the electrocatalyst was filtered and dried at 80^0 C overnight. The TEM image shows the good distribution of the catalyst on the carbon support.

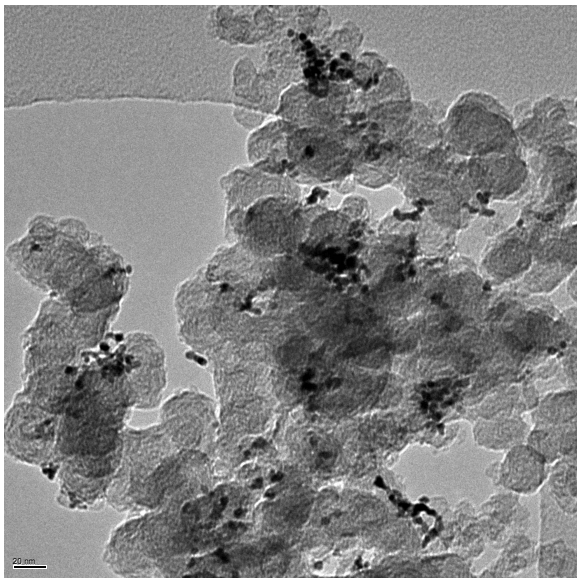

Figure S6 – TEM image of the PtSn (1:1) nanoparticles.

References

[1] M.C. Figueiredo, O. Sorsa, N. Doan, E. Pohjalainen, H. Hildebrand, P. Schmuki, B.P. Wilson, T. Kallio, Direct alcohol fuel cells: Increasing platinum performance by modification with sp-group metals, Journal of Power Sources, 275 (2015) 341-350.

[2] N.M. Cantillo, J. Solla-Gullón, E. Herrero, C. Sánchez, Ethanol Electrooxidation on PtSnNi/C Nanoparticles Prepared in Water-In-Oil Microemulsion, ECS Transactions, 41 (2011) 1307-1316.